

n-HEXANE ISOMERIZATION OVER NICKEL-CONTAINING MORDENITE ZEOLITE

Lyubov Patrylak¹, ✉, Mariya Krylova¹, Oleksandra Pertko¹,
Yuliya Voloshyna¹, Angela Yakovenko¹

<https://doi.org/10.23939/chcht14.02.234>

Abstract. Nickel-containing mordenite samples were synthesized by impregnation from aqua's solution of nickel nitrate. Porous and catalytic characteristics of the catalysts were studied by means of low temperature nitrogen adsorption/desorption and micropulse *n*-hexane isomerisation. The maximum isomer yields are 10-12 wt % for 1-5 wt % Ni content at 523–573 K.

Keywords: *n*-hexane isomerization, mordenite zeolite, activity, nickel, palladium, activity, selectivity.

1. Introduction

The isomerization of *n*-alkanes is a process of great importance for the oil refining industry. This reaction transforms linear alkanes into branched ones, which have higher octane numbers and therefore utilize light gasoline fraction of atmosphere refining [1-6]. Usually, branched paraffins are obtained by isomerization over bifunctional catalysts, which have Brønsted and Lewis acidic and hydrogenating-dehydrogenating active sites [7-11]. Mordenite zeolite and alumina are used in the role of acidic support, whereas hydrogenating-dehydrogenating sites are usually formed by platinum group metals. Alumina based catalysts are the low temperature (403–448 K) ones and those on the basis of mordenite zeolite – the middle temperature (523–573 K) ones. Each of them has its advantages and disadvantages. The first type of catalysts, the chlorinated platinum-loaded alumina, despite the higher yields of branched isomers is very sensitive to admixtures (water, sulfur compounds). The second type of catalysts has low sensitivity to water and sulfur. The relatively high costs of platinum group metals make both types of catalysts very expensive. In the role of isomerization catalysts the superacids based on zirconium

oxide can also be used [8, 11]. Nickel, being a *d*-element, is in the same group with palladium and platinum in periodic table, and demonstrates hydrogenating-dehydrogenating properties. A number of researchers investigated bimetallic Ni-Pt zeolite isomerization catalysts [12-15]. It was also found [16] that zeolite ZSM-5 doped by nickel exhibits good parameters in isomerization of linear alkanes.

Therefore, the aim of the present work was the investigation of nickel-containing isomerisation catalysts on the basis of synthetic mordenite zeolite.

2. Experimental

Zeolite catalyst samples have been synthesized on the basis of NaM zeolite ($\text{SiO}_2/\text{Al}_2\text{O}_3 = 9.8$, produced by JS “Sorbent”, Nizhny Novgorod, Russia). H-form zeolite (HM) has been obtained by threefold ion exchange of native sodium cations for NH_4^+ from ammonium nitrate NH_4NO_3 aqueous solution (3 mol/l). Ion-exchange duration was performed at 358 K for 3 h, followed by calcination in air (823 K, 2 h). Nickel impregnation was applied from nickel nitrate solution (0.6 mol/l) in an amount of 1, 5 and 15 wt %. The solution was evaporated on a sand bath for 3 h and dried at 373 K for 2 h. Then the samples were kept for 6 h in a stream of hydrogen at 653 K to the nickel reduction to the null valence state. As a result, the samples NiHM-1, NiHM-5 and NiHM-15 with 1, 5 and 15 wt % of Ni, respectively, have been obtained.

The adsorption/desorption isotherms of the synthesized samples have been investigated *via* low-temperature (77 K) nitrogen adsorption/desorption using Quantachrome Autosorb NOVA 1200e porometer. Parameters of the porous structure were calculated using the software NOVWin™. The specific surface areas (S^{BET}) have been calculated according to the BET method utilizing the nitrogen adsorption data at P/P_s values between 0.06 and 0.2. The micropores volumes (V_{micro}^t) and micropores surface areas (S_{micro}^t) have been estimated using the de Boer *t*-plot method.

X-ray diffraction studies used a standard XRD measurement on DRON-4-07 diffractometer with the Ni

¹ V.P. Kukhar Institute of Bioorganic Chemistry and Petrochemistry of National Academy of Sciences of Ukraine
1, Murmans'ka St., 02660 Kyiv, Ukraine

✉ lkpg@ukr.net

© Patrylak L., Krylova M., Pertko O., Voloshyna Yu., Yakovenko A., 2020

filtered CuK α radiation in a reflected beam at the Bragg-Brentano focus geometry in the range of $2\theta = 5\text{--}80^\circ$ with a step of 0.05 and 1 s exposure. Individual intervals were recorded with a step of 0.02 degree and an exposure of 4 s. The phase composition of the samples was determined using the X-ray diffraction data base PDF-2, ICDD, Newton Square, PA. The average size of nickel crystallites was determined from the (111) and (200) X-ray lines broadening utilizing the Scherrer's formula.

Catalytic investigations have been carried out at the laboratory setup with a microreactor. Such testing technique allows to minimize the reaction time on the catalyst bed and to obtain primary transformation products [17], which is useful for reflection on the mechanisms of reactions [17-19].

Catalyst efficiency has been studied in the linear hexane isomerization utilizing the micropulse setup based on gas chromatograph TSVET-104 equipped with a flame ionization detector [20]. High purity hydrogen was used as a carrier gas. The reaction was studied in the temperature range from 473 to 573 K. Linear hexane has been dosed by pulses of 1 μl using a microsyringe in the top of the reactor. The products and unconverted *n*-hexane were collected in a cooled by liquid nitrogen (77 K) trap connected with the reactor bottom and analyzed online using a capillary column (50 m, 0.25 mm inner diameter) with a squalane as the stationary phase after vaporizing by a thermal impulse of 473 K. The temperature in the column thermostat was 323 K.

3. Results and Discussion

The low temperature adsorption/desorption nitrogen isotherms for the synthesized samples are shown in Fig. 1. On their basis porous characteristics of the samples have been calculated and summarized in Table 1.

Isotherms are typical ones for micro/mesoporous sorbents, which are characterized by a steep rise at low P/P_s values assigned to the formation of equilibrium Langmuir adsorbate monolayers and a hysteresis loops over higher P/P_s values [21-24]. Isotherms belong to IVa type with H3 hysteresis loop according to the classification of IUPAC [21], and this could be related to cylindrical pore channels. The shape of the isotherms and the hysteresis loops both indicate adsorption not only in the micropores, but also on the outer surface of the

crystals and mesopores. The presence of the hysteresis loops demonstrates the implementation of capillary condensation in the mesopores that arose not in the result of impregnation by nickel but during the deactivation process. In Fig. 2 the differential pores size distribution for investigated samples calculated by DFT method is depicted. The wideporous mordenite type zeolite has two types of microporous channels: 0.29×0.57 and 0.65×0.7 nm. In addition, mesopores with a radius of about 1 nm and 2–3 nm are clearly visible in Fig. 2. They are practically not changed in the process of nickel impregnation.

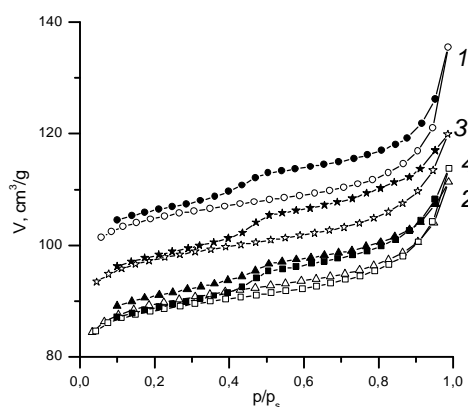


Fig. 1. Low temperature nitrogen adsorption/desorption isotherms for the prepared samples on the basis of synthetic mordenite: HM (1), NiHM-1 (2), NiHM-5 (3) and NiHM-15 (4)

For all catalysts, a slight decrease in the total pore volume due to impregnation has been observed. A sample with 1 wt % of nickel is characterized by the largest decrease of the micropore surface area after impregnation. Probably, this is due to the minimal size of nickel particles that blocked more inputs into the mordenite channels.

The analysis of X-ray diffraction patterns for synthesized samples (Fig. 3) shows that all catalysts have a crystalline structure corresponding to the structure of MOR zeolite (JCPDS Card # 29-1257) [24]. XRD phase of mordenite is found to match with the peaks at $2\theta = 6.51, 9.77, 18.07, 20.34, 26.14, 28.89, 30.39, 37.00, 38.92, 39.75, 40.55, 41.90, 42.62, 44.68, 46.94, 47.98, 48.85$ and 49.59 . These peaks are characteristic for mordenite zeolite, and correspond to the planes (110), (200), (131), (041), (060), (441), (531), (711), (133), (570), (480), (423), (082), (063), (911), (173), (114) and (204).

Table 1

Porous characteristics of the catalysts on the basis of mordenite zeolite

Sample	$S^{BET}, \text{m}^2/\text{g}$	$S^t_{micro}, \text{m}^2/\text{g}$	$V_{\Sigma}, \text{cm}^3/\text{g}$	$V^t_{micro}, \text{cm}^3/\text{g}$	Average pore radius, nm
HM	382	365	0.21	0.16	1.10
NiHM-1	336	319	0.17	0.13	1.02
NiHM-5	360	342	0.19	0.14	1.03
NiHM-15	328	310	0.18	0.13	1.07

Three characteristic peaks for nickel ($2\theta = 44.5^\circ$, 51.8° , and 76.4°), corresponding to Miller indices (111), (200), and (222), are also shown in Fig. 3. The latter line (222) is of the lowest intensity. The intensity of peaks increases with the increase of nickel content in the samples. The appearance of these peaks reveals that the resultant particles are pure facecentred cubic nickel at these samples (JCPDS, No. 04-0850). Unfortunately, for small amounts of nickel (1 wt %), it was difficult to isolate the reflexes to calculate the size of its particles due to the overlap of zeolite and nickel lines, but its presence in the NiHM-1 sample indicates a change in the intensity

of the line (111) and an increase in the background level in comparison with a sample of HM (Fig. 4). For the samples of NiHM-5 and NiHM-15, in addition to crystalline nickel reflexes, even more background elevations are observed.

The average size of nickel particles for samples NiHM-5 and NiHM-15 was 20 and 22 nm, respectively (Ni cubic, JCPDS Card #4-850). Based on the received pore size distribution for the investigated zeolites and the size of the nickel particles, we can talk about the localization of the latter only on the outer surface of the zeolite crystals.

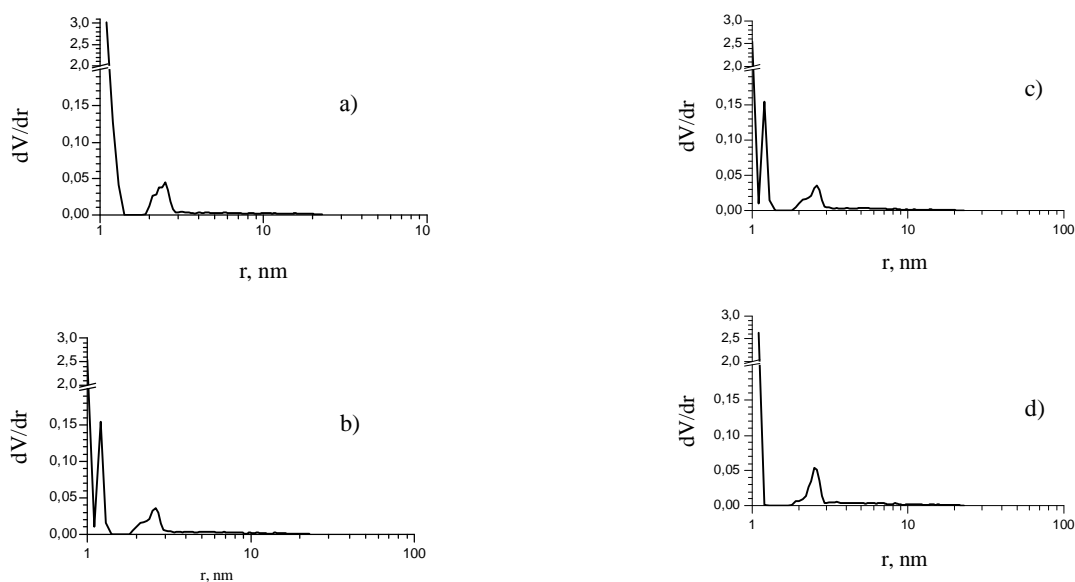


Fig. 2. Differential pore size distributions calculated by DFT method for HM (a), NiHM-1 (b), NiHM-5 (c) and NiHM-15 (d) samples

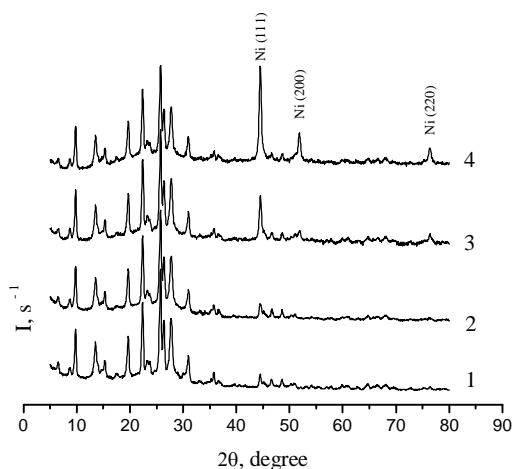


Fig. 3. X-ray powder diffraction patterns of HM (1) and nickel-containing mordenite catalysts NiHM-1 (2), NiHM-5 (3) and NiHM-15 (4)

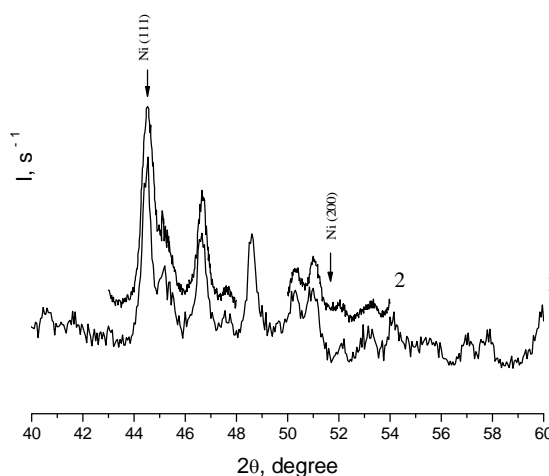


Fig. 4. Fragments of X-ray powder diffraction patterns of HM (1) and 1 wt % nickel-containing mordenite catalysts NiHM-1 (2)

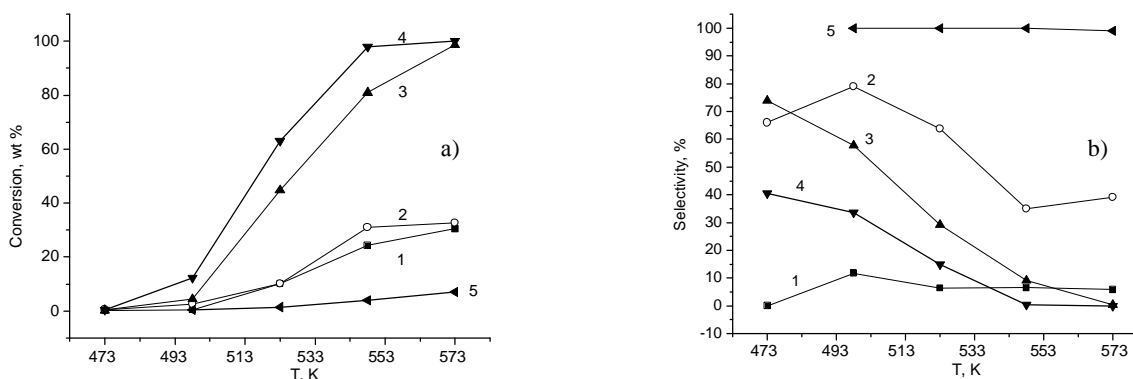


Fig. 5. *n*-Hexane conversion (a) and isomers selectivity (b) for HM (1), NiHM-1 (2), NiHM-5 (3), NiHM-15 (4) and PdHM (5) samples

Table 2

Yields of isomerization products in micro pulse linear hexane isomerization over Ni-containing mordenite samples

Sample	Yield at different temperatures, wt %			
	498 K	523 K	548 K	573 K
HM	1.0	1.5	2.0	2.0
NiHM-1	2.0	5.0	10.0	11.0
NiHM-5	2.0	12.0	6.0	1.0
NiHM-15	4.0	8.0	1.0	0.5

Among the products of isomerization of *n*-hexane there are both isomers *i*C₆ and cracking products C₁-C₅. Conversion over the samples on the basis of mordenite (Fig. 5a) strongly depends on the content of hydrogenating-dehydrogenating components and increases with its increase for the catalysts with 1, 5 and 15 wt % of nickel. Thus, at 548 K this increase ranges from ~25 to 75 and 100 wt %, respectively. Catalyst with 1 wt % Ni converts at the level of the original HM sample. But impregnation of 1 % of Ni causes a sharp increase in catalyst selectivity for hexane isomers (Fig. 5b), which remains the highest among four samples within the temperature range. As a result, regarding the isomers yield (Fig. 5), this catalyst is not inferior to other nickel-containing samples, but its maximum value is achieved at the temperature by 25–50 K higher than that for the catalysts with higher nickel content. This is obviously due to high activity of latter ones relative to hexane conversion. The increase in temperature increases the catalysts selectivity relative to cracking products (Fig. 5b) and they become unable to maintain a high yield of the target products. For comparison in Fig. 5 the results obtained over palladium-containing mordenite [20] are shown. This catalyst is characterized by a high selectivity at relatively low activity.

Thus, at 523–573 K the highest yield of hexane isomers (Table 2) on the mordenite based samples is 10–12 wt % for Ni content of 1–5 wt %.

Since a spatially close combination of the Brønsted and Lewis acid centers, as well as the hydrogenating-dehydrogenating centers (metal nickel in our case), is necessary for the realization of linear hydrocarbon structures isomerization, the conversion obviously occurs not in the micropores of zeolite, but on the external surface of the crystals. The latter is relatively small ($S_{ex} = S^{BET} - S_{micro}^t = 17-18 \text{ m}^2/\text{g}$, Table 1). The resulting yields are smaller than those observed over Ni-containing pentasil zeolites (up to 20–25 % [16], for which it was possible to obtain nickel particles with smaller size from 8–9 to 16–18 nm. Therefore, in order to raise the yields, it is expedient, firstly, to expand the pore size of the mordenite, for example, by carrying out an additional dealumination of the zeolite lattice, and, secondly, to reduce the size of the impregnated metal particles.

Thus, the sample with the best ratio of the selectivity/activity parameters is NiHM-5, and the optimum isomerization temperature is 523 K. The NiHM-1 catalyst, showing similar yields, requires temperatures higher by 25–50 K. The characteristics of these samples are the closest to the isomerization results over palladium-containing mordenite [20].

Acknowledgments

The authors express their gratitude to the senior researcher Olena I. Oranska, PhD, leading engineer Yuriy I. Gornikov (O.O. Chuiko Institute of Surface Chemistry,

NAS of Ukraine) for conducting an X-ray diffraction analysis of the samples, and leading engineer Dmytro V. Molodyi (V.P. Kukhar Institute of Bioorganic Chemistry and Petrochemistry, NAS of Ukraine) for adsorption measurements.

The publication contains the results achieved due to the grant of the President of Ukraine on competitive projects F74/179-2017 of the State Fund for Fundamental Research.

References

- [1] Primo A., Garcia H.: Chem. Soc. Rev., 2014, **43**, 7548. <https://doi.org/10.1039/C3CS60394F>
- [2] Liu S., Ren J., Zhang H. et al.: J. Catal., 2016, **335**, 11. <https://doi.org/10.1016/j.jcat.2015.12.009>
- [3] Dhar A., Vekariya R., Sharma P.: Petroleum, 2017, **3**, 489. <https://doi.org/10.1016/j.petlm.2017.02.001>
- [4] Izutsu Y., Oku Y., Hidaka Y. et al.: Catal. Lett., 2013, **143**, 486. <https://doi.org/10.1007/s10562-013-0973-y>
- [5] Ghouri A., Usman M.: J. Chem. Soc. Pak., 2017, **39**, 919.
- [6] Dhar A., Vekariya R., Bhadja P.: Cogent Chem., 2018, **4**, 1514686. <https://doi.org/10.1080/23312009.2018.1514686>
- [7] Dhar A., Dutta A., Castillo-Araiza C. et al.: Int. J. Chem. Reactor Eng., 2016, **14**, 795. <https://doi.org/10.1515/ijcre-2015-0052>
- [8] Tamizhdurai P., Lavanya M., Meenakshisundaram A. et al.: Adv. Por. Mater., 2017, **5**, 169. <https://doi.org/10.1166/apm.2017.1127>
- [9] Yun S., Seong M., Park Y. et al.: J. Nanosci. Nanotechnol., 2015, **15**, 647. <https://doi.org/10.1166/jnn.2015.8328>
- [10] Patrylak L.: Adsorpt. Sci. Technol., 1999, **17**, 115. <https://doi.org/10.1177/026361749901700205>
- [11] Brei V.: Theor. Experim. Chem., 2005, **41**, 165. <https://doi.org/10.1007/s11237-005-0035-7>
- [12] Yoshioka C., Garetto T., Cardoso D.: Catal. Today, 2005, **107-108**, 693. <https://doi.org/10.1016/j.cattod.2005.07.056>
- [13] Jordao M., Simoes V., Cardoso D.: Appl. Catal. A, 2007, **319**, 1. <https://doi.org/10.1016/j.apcata.2006.09.039>
- [14] Lima P., Garetto T., Cavalcante C.L.Jr. et al.: Catal. Today, 2011, **172**, 195. <https://doi.org/10.1016/j.cattod.2011.02.031>
- [15] Martins G., dos Santos E., Rodrigues M. et al.: Modern Res. Catal., 2013, **2**, 119. <https://doi.org/10.4236/mrc.2013.24017>
- [16] Patrylak L., Krylova M., Pertko O. et al.: J. Porous Mater., 2019, **26**, 861. <https://doi.org/10.1007/s10934-018-0685-1>
- [17] Patrylak L.: Adsorpt. Sci. Technol., 2000, **18**, 399. <https://doi.org/10.1260/0263617001493512>
- [18] Patrylak K., Patrylak L., Repetskyi I.: Theor. Experim. Chem., 2013, **49**, 143. <https://doi.org/10.1007/s11237-013-9308-8>
- [19] Patrylak K., Patrylak L., Voloshyna Yu. et al.: Theor. Experim. Chem., 2011, **47**, 205. <https://doi.org/10.1007/s11237-011-9205-y>
- [20] Patrylak L., Manza I., Vypirailenko V. et al.: Theor. Experim. Chem., 2003, **39**, 263. <https://doi.org/10.1023/A:1025729530977>
- [21] Rouquerol F., Rouquerol J., Sing K.: Adsorption by Powders and Porous Solids. Principles, Methodology and Applications. Academic Press, San Diego 1999.
- [22] Patrylak L., Likhnyovskiy R., Vypyraylenko V. et al.: Adsorpt. Sci. Technol., 2001, **19**, 525. <https://doi.org/10.1260/0263617011494376>
- [23] Patrylak L.: Zh. Phys. Khim., 2005, **79**, 1658.
- [24] Smail H., Shareef K., Ramli Z.: Austral. J. Bas. Appl. Sci., 2017, **11**, 27. <http://www.ajbasweb.com/old/ajbas/2017/January/27-34.pdf>

Received: October 08, 2018 / Revised: October 31, 2018 / Accepted: January 28, 2019

ІЗОМЕРИЗАЦІЯ Н-ГЕКСАНУ НА НІКЕЛЬВМІСНОМУ ЦЕОЛІТІ ТИПУ МОРДЕНІТУ

Анотація. Синтезовано зразки нікельвмісного морденіту внаслідок просочування із водних розчинів нітрату нікелю. З використанням методу низькотемпературної адсорбції/десорбції азоту та мікроімпульсної ізомеризації н-гексану вивчено пористі та каталітичні властивості. За температур 523–573 К максимальні виходи ізомерів становлять 10-12 % мас. для вмісту Ni 1–5 % мас.

Ключові слова: ізомеризація н-гексану, цеоліт типу морденіту, нікель, паладій, активність, селективність.